J. Physiol. (1953) 122, 429–461

INTRACELLULAR RECORDING FROM ANTIDROMICALLY ACTIVATED MOTONEURONES

By L. G. BROCK, J. S. COOMBS and J. C. ECCLES

From the Departments of Physiology, University of Otago, New Zealand, and the Australian National University, Canberra, Australia

(*Received* 15 *May* 1953)

For more than two decades there has been an intensive investigation of the effects produced on a motoneurone by an impulse that propagates antidromically up its motor axon. A fairly comprehensive reference to these investigations was made in two recent publications (Barakan, Downman & Eccles, 1949; Brooks, Downman & Eccles, 1950), and since then a further intensive study has been reported by Lloyd (1951*a*, *b*). Despite all this investigation there has been a failure to reach general agreement on the many fundamental issues listed below:

(i) Lorente de Nó (1947) concluded that the spike potential of the soma or cell body was briefer than that of the axon, while Barakan *et al.* (1949) and Eccles (1950) concluded that it was considerably longer. It will appear that Lloyd (1951*a*) also supports this latter conclusion, for it will be argued below that his deflexion '*d*' in part arises in the soma.

(ii) Renshaw (1942) and Lorente de Nó (1947) concluded that the propagation of an antidromic impulse was usually blocked in its propagation over the dendrites and not at the axon–soma junction, whereas Lloyd (1943), Barakan *et al.* (1949) and Eccles (1950) concluded that this junction was the usual site of blockage, and, having traversed this region, an antidromic impulse was not usually blocked until it reached the dendritic terminals. Barakan *et al.* (1949) have further reported that there is an axon–soma delay of 0·1–0·3 msec due to the very slow antidromic propagation at the axon–soma junction. However, recently Lloyd (1951*a*) has proposed a compromise in that axon–soma blockage is not explicitly denied, but emphasis is laid on blockage during conduction along the dendrites.

(iii) Eccles & Pritchard (1937), Gasser (1939) and Brooks *et al.* (1950) reported that, when invaded by an antidromic volley, motoneurones developed a much larger positive after-potential than axons, the motoneurones as a consequence being relatively positive to their axons (in the external circuit)

for 100 msec or more. In partial contradistinction Lloyd (1951*b*) has concluded that after about 45 msec the axonal positive after-potential was larger than that of the soma, so that there was a reversal of current flow in the external circuit. This conclusion led to the development of explanations for the excitability cycles of the axons and somas of invaded motoneurones, and also of the adjacent motoneurones whose axons had not been stimulated (cf. Renshaw, 1942).

(iv) Brooks *et al.* (1950) reported that, a few milliseconds after antidromic activation of a motoneurone pool, some at least of those motoneurones were more excitable than at the depth of depression about 10 msec later; this was confirmed by Lloyd (1951*a*). In part at least this effect was attributed to a brief waning phase of supernormal excitability in motoneurones which had been partly depolarized by antidromic impulses that had been blocked at their axon–soma junctions. But the effect was also in part attributed to a negative after-potential of the invaded motoneurones. On the other hand, Lloyd (1951*b*) rejected both these explanations in favour of a postulated outward flow of current from the soma to the axon which was shown to be in a state of negative after-potential, at least in the extramedullary segment.

Such differences in the description of events occurring during antidromic invasion of a motoneurone undoubtedly arise because of the difficulty in interpreting the complex potential fields that are generated at all stages of the invasion and subsequently. The antidromic volley would be propagating into thousands of motoneurones with their densely interlacing dendrites, but the potential picked up by an extracellular micro-electrode would be predominantly generated by the few adjacent neurones (cf. Barakan *et al.* 1949; Eccles, 1950). In contrast, an intracellular electrode will record the potentials generated by one motoneurone to the virtual exclusion of all others (Brock, Coombs & Eccles, 1951, 1952*a*). By systematic study of the responses of some sixty motoneurones under a wide variety of experimental procedures, it has been possible to give a detailed description of the events occurring during antidromic invasion of a motoneurone, and thus incidentally to produce evidence relating to most of the above controversial issues. In addition, the electrical potentials generated by repetitive antidromic activation have been studied. The properties of the motoneurone, as determined in this investigation, will form a basis for the explanation of synaptic excitatory and inhibitory actions in subsequent papers. Brief preliminary accounts have already been published (Brock, Coombs & Eccles, 1953; Eccles, 1953).

Cats were used, as has been fully described in a recent paper (Brock *et al.* 1952*a*), which also gives a description of the spike potential set up by antidromic invasion of a motoneurone (cf. also Brock *et al.* 1951). The rather complex geometrical conditions encountered by an antidromic impulse make it expedient to preface the experimental results by brief accounts of the anatomical pathway traversed by an antidromic impulse and of an hypothesis which purports to give the simplest explanations of the antidromic invasion of a motoneurone.

THE ANATOMY OF THE ANTIDROMIC PATH

As traced upwards from the motor nerve, a motor axon runs with an approximately uniform diameter and with approximately uniform conditions of myelination until, as a fibre of the ventral root, it has entered the spinal cord, passed through the white matter and penetrated some distance within the grey matter of the ventral horn (Fig. 1A; Cajal, 1909). There is then a sudden loss of the myelin sheath and the non-medullated segment of the axon extends usually for 50–100 μ before expanding to join the soma of a motoneurone in the conically expanded axon hillock (Fig. 1B). Much of the non-medullated segment is very constricted, giving the so-called 'thin segment' (cf. Fig. 1A; Brock *et al.* 1952*a*). Since it may be assumed that the antidromic impulse traverses the surface of the neurone, its subsequent course will be from the axon hillock over the surface of the soma and thence up the dendrites and along their numerous branches to their profuse terminal arborizations.

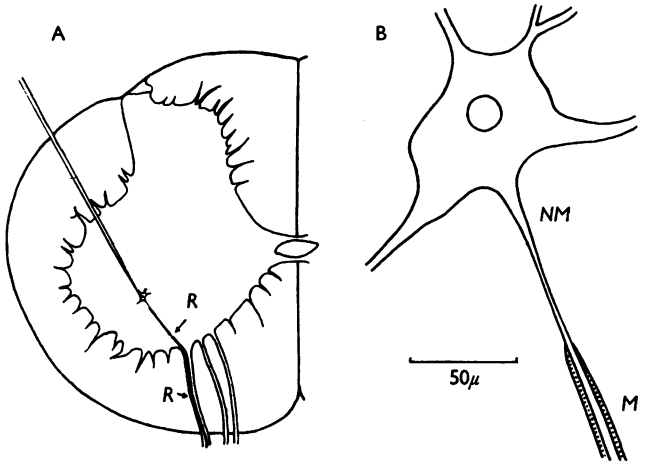

Fig. 1. Drawings showing pathway of antidromic impulse invading motoneurone. A: transverse section of spinal cord showing typical path of axon to motoneurone in the biceps-semitendinosus nucleus, and the nodes of Ranvier, *R* (shown in exaggerated form) that occur in its medullated segment, which is shown penetrating the grey matter and ending within 100 μ of the axon–soma junction. Note also micro-electrode in position. B: tracing from a photomicrograph of an actual motoneurone (cf. Brock *et al.* 1952*a*, fig. 1A), which shows in particular the beginning of the medullated segment, *M* (shown stippled) the non-medullated segment, *NM*, with the thin segment and the axon hillock.

PRELIMINARY HYPOTHESIS OF ANTIDROMIC INVASION

The simplest assumption is that the propagation of the antidromic impulse occurs by the well-established local-current mechanism (cf. Lorente de Nó, 1947; Brooks & Eccles, 1948; Barakan *et al.* 1949). As a consequence special features are introduced where the axon loses its myelin sheath and where there is a large increase in the surface area of the membrane being invaded by the impulse. In the former situation the safety factor for propagation would be expected to be low because there would be a large increase in the area of membrane that was being depolarized by the inward sodium current through

the adjacent active nodes (Huxley & Stämpfli, 1951). In the latter situation an expansion of the surface area, as for example at the axon–soma junction, would likewise lower the safety-factor for a similar reason. This expansion would also be an important factor in propagation along the profusely branching dendrites. Apart from such geometrical factors, it is assumed in this preliminary hypothesis that the surface membrane is otherwise the same over the whole neurone; for example, that uniformity prevails for the capacity, ionic conductance, resting potential and the critical depolarization at which a self-regenerative depolarization is initiated.

Thus, on the basis solely of the geometrical features of the system, it would be expected that antidromic impulses encounter three zones of specially difficult propagation: at the medullated–non-medullated junction; at the axon–soma junction; and at the profusely branching dendritic terminals. It would be predicted that antidromic propagation would be momentarily delayed or slowed at these regions, or even blocked. Furthermore, it would be predicted that propagation through these difficult zones would be aided by depolarization of the region beyond and impeded by its hyperpolarization.

RESULTS

I. *The action-potential of the non-medullated axon*

When an antidromic impulse has invaded a motoneurone, setting up the characteristic spike action potential (Brock *et al.* 1951, 1952*a*), there has invariably been a brief step or double inflexion on the rising phase of the spike at a voltage of about 30–40% of the spike potential. Fig. 2 shows a series of such spike action potentials for different motoneurones in which the delay on

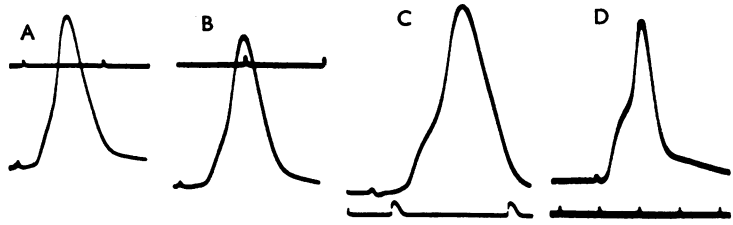

Fig. 2. Intracellular records of potentials generated by a single antidromic impulse in four different motoneurones. As shown by millisecond scale, records A, B and C have a much faster time scale than record D. The time line approximately signals the resting potential in A and B, which was 64 and 76 mV respectively.

the rising phase varied from about 0·05 msec in record A to 0·3 msec in record D. This delay is approximately measured as the forward advance of the second phase which is necessary to eliminate the inflexion. In the experiment that gave the longest delay (Fig. 2D), the neuronal spike often failed to develop (in eight of the nineteen responses that were photographed), and there was

consequently merely a simple brief spike with a voltage of about 40% of the neuronal spike (Fig. 3A). Finally, with many motoneurones an antidromic impulse always set up a simple brief spike of relatively low voltage which had no sign of a double inflexion on the rising phase (Figs. 3B, C).

These simple spike potentials were invariably set up by an antidromic impulse a few milliseconds after a conditioning antidromic impulse (see § II*b*, p. 437), while at longer intervals the full neuronal spike was observed, though with

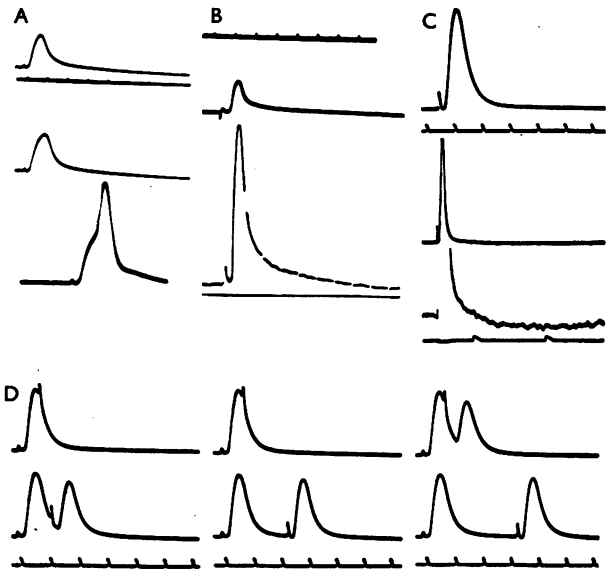

Fig. 3. Intracellular action potentials evoked by single antidromic impulses as in Fig. 2. A: three responses at intervals of a few seconds to illustrate the small simple spikes and the double spike in the same neurone; time, msec. B: shows, with another motoneurone, the same small spike (27 mV) recorded at low and high amplification; time, msec. C: three records of the same small simple spike (about 35 mV) the first being at a much faster time scale, 1 msec, than the other two (cf. lower scale, 10 msec), and the last at ten times the amplification of the first two. D: same neurone as C, but for two stimuli applied at progressively longer intervals; time scale in milliseconds.

a lengthening of the delay in the rising phase (cf. Fig. 5A). On the other hand, conditioning by a preceding volley has failed to reveal any double inflexion on the rising phase of the small simple spikes illustrated in Figs. 3 and 12 (cf. Fig. 3D).

The small simple spikes have also differed from the fully developed neuronal spike in that they had a much smaller positive after-potential. In Fig. 3C the positive after-potential is seen to decline after reaching its maximum at about 10 msec. The full time course is seen in Fig. 12, and is particularly evident for the larger after-potentials that follow the repetitive simple spikes. The

invariable value of less than 1·0% of the small spike potential contrasts with values from 3 to 10% (mean 4·5%) for the positive after-potential that follows the large spike (Brock *et al.* 1952*a*). On the other hand, a considerable after-negativity was usually present. As a consequence (cf. Fig. 3 A and B, but not C) the end of the spike has been hard to define because it has merged into an after-negativity that has slowly decayed over several milliseconds (cf. § II *b* (2), p. 443).

Discussion. In view of the antidromic transmission properties expected for a motoneurone, the above experimental evidence immediately suggests that the small simple spike is set up by an antidromic impulse that has traversed the non-medullated segment of the axon, but has failed to invade the soma and dendrites. An impulse in this segment would be expected to give a simple brief spike of all-or-nothing character and with the small positive after-potential that is characteristic of the mammalian axon (Gasser & Grundfest, 1936). The double inflexion between this initial spike and the main antidromic spike would then be attributable to a delay of 0·05–0·3 msec between the arrival of the axonal spike at the axon–soma junction and the initiation of the soma spike (as postulated by Barakan *et al.* 1949). However, it may seem improbable that a micro-electrode in a neurone would record such a large spike (30–40 mV) from its relatively small axonal process. It is thus necessary to consider in detail the propagation of an antidromic impulse and the manner in which intracellularly recorded potentials arise.

As an antidromic impulse passes up the axon hillock, it would be confronted by a very rapid expansion of the membrane to be invaded (cf. Fig. 1 B); hence there would be a grave lowering of the safety factor for propagation, which would be expected to be at a minimum somewhere about a region marked '*X*' in Fig. 4 A. That is, once an antidromic impulse passed '*X*' it would rapidly invade the rest of the soma and dendrites, but on the other hand it could be extinguished before passing '*X*', and hence give, as postulated, the small simple spike. As shown in Fig. 4 A, when an antidromic impulse is propagating up to the axon hillock, there will be a current from the soma–dendritic membrane into the region of intense inward current across the activated membrane of the axon hillock and non-medullated axon. This current will tend rapidly to depolarize the soma–dendritic membrane. However, the magnitude of this depolarization will be less than the simultaneously recorded intracellular potential by the voltage drop that occurs along the line of current flow from the intracellular electrode outwards across the soma–dendritic membrane to the equipotential surface at earth potential (cf. Fig. 4 A). The external component of this voltage is no more than about 2mV when it is recorded by a micro-electrode that is inserted to a position just short of penetrating the motoneurone. The internal component is at present indeterminate, but, on account of the relatively restricted internal current pathways, it is probably

considerably larger than the external component. Nevertheless, the actual depolarization of the soma–dendritic membrane would be about 30 mV when the small spike potential is at its usual value of 30–40 mV, which is just critical for generating the soma–dendritic spike (cf. Figs. 2, 3A, 5A, 8 and 9). In particular, a very large depolarization would be expected for those parts of the soma membrane close to the region (Fig. 4A) at which the antidromic impulse is blocked.

There is thus convincing evidence that a depolarization of about 30 mV is just critical for the generation of an impulse by antidromic invasion of a soma membrane. This value is much greater than the critical level (about 10 mV) at

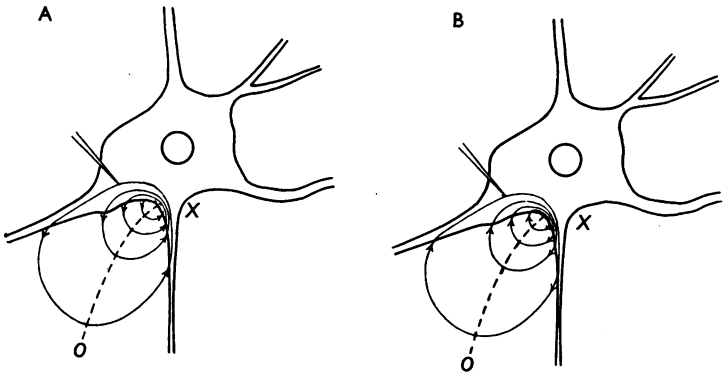

Fig. 4. A: drawing of motoneurone showing postulated lines of current flow during the rising phase of the small simple spike. The isopotential line at earth potential is drawn orthogonally and marked *O*. B: as in A, but during the falling phase of the small simple spike. The rapid repolarization of the active membrane causes it to act as a source in the external circuit, so aiding in repolarization of the soma–dendritic membrane.

which a post-synaptic potential causes the generation of an impulse (Brock *et al.* 1952*a*; Eccles, 1952, 1953). The discrepancy may be explained by taking account of the subsequent events in the two situations.

During the recovery phase of the antidromic impulse in the axon and axon hillock there will be a rapid repolarization due to the intense outward potassium current (Hodgkin & Huxley, 1952*a*, *d*). As a consequence this region carrying the intense outward current will rapidly become more polarized than the soma–dendritic membrane, and the direction of current flow will reverse as shown in Fig. 4B. Thus, on cessation of the initial depolarizing current, the soma–dendritic membrane will be repolarized by the conjoint effects of two currents; the extrinsic current from the axon and axon hillock; the intrinsic current of the membrane due largely to the unbalanced flux of potassium and chloride ions. With small depolarizations this latter current would repolarize the membrane capacity with a time course approximately given by the resting time constant of the membrane, which has been indirectly measured as 4 msec to repolarize to $1/e$ of the initial value (Brock, Coombs & Eccles, 1952*b*; Eccles, 1952, 1953). For example, with all sizes of post-synaptic potentials, i.e. up to 10 mV or even more, the membrane repolarization occurs with a time constant of about 4 msec and is satisfactorily attributable to the unbalanced resting ionic flux. However, with the small spike the depolarization presumably will be sufficiently large to

cause a substantial increase in potassium permeability (Hodgkin & Huxley, 1952*a*) and hence the time constant of repolarization due to the intrinsic current will be considerably less than 4 msec. In part, this intrinsic current will account for the decline of the small spike, particularly in the later stages where the time constant is as long as 3 msec (Fig. 3A, B). However, it is suggested that the early rapid decline of the small spike would be largely attributable to the extrinsic current flow. In contrast there is no evidence that an extrinsic repolarizing current occurs during the post-synaptic potential.

The extrinsic repolarizing current provides an explanation of the large discrepancy between the membrane depolarizations at which a soma–dendritic spike is generated by orthodromic and antidromic activation respectively. In the absence of extrinsic repolarizing current the critical depolarization is about 10 mV, which may be regarded as a reliable value for the membrane depolarization at which a self-regenerating sodium carrier activity is initiated, i.e. the threshold for an impulse. It has been shown by Hodgkin & Huxley (1952*b*) that in the squid giant axon the sudden application of a repolarizing current by a voltage clamp very effectively and quickly quenches any sodium-carrier activity that may have developed in response to a depolarization. If the extrinsic repolarizing current exerts this quenching effect on the soma–dendritic membrane, the much larger depolarization (about 30 mV—a threefold increase) necessary for generating an impulse antidromically may be accounted for. Presumably the soma–dendritic depolarization is not all attributable to the flow of extrinsic currents into the activated membrane of the axon and axon hillock (Fig. 4A), for after a certain level of depolarization it would be expected that the increased sodium conductance of the soma–dendritic membrane would cause a significant contribution from an intrinsic current, i.e. there would be a local response of the membrane (cf. §II*b* (2); Hodgkin & Huxley, 1952*a*, *d*).

The attribution of the small simple spike to the antidromic invasion of the non-medullated axon plus axon hillock, and the large 'neuronal' spike to the antidromic invasion of the soma and dendrites, has been supported by much evidence to be presented in this and subsequent papers (Brock *et al.* 1952*b*). It is therefore proposed henceforth to designate the small simple spike 'the *NM* spike' (non-medullated spike), and the large spike 'the *SD* spike' (soma–dendritic spike). The delay in the transition between these two spikes would give an approximate measure of the axon–soma delay. Although the *NM* spike would be generated primarily by the response of the non-medullated axon and axon hillock, it is important to remember that it is recorded from the soma region, and therefore registers potentials produced secondarily in the soma–dendritic membrane. Consequently, the *NM* spike gives not only a diminished (from say 100 to 40 mV) but also a distorted record of the spike actually occurring in the non-medullated segment. This distortion is particularly evident in the prolonged after-negativity following many *NM* spikes (Fig. 3A–B), an effect attributable to the residual depolarization of the soma–dendritic membrane which decays along a time course largely determined by the time constant of this membrane in the resting state. As illustrated in Fig. 3C some *NM* spikes show little trace of this delayed decline, which may be explained by the micro-electrode being located close to the axon hillock and hence recording relatively undistorted *NM* spikes. Another type of distortion would be produced by any local response that may occur in the soma–dendritic membrane (Fig. 3A).

II. *Action potentials generated by a second antidromic impulse*

(*a*) *After an NM spike*

Fig. 3D shows a typical series of responses with progressively increasing stimulus interval. With intervals less than 0·82 msec the second stimulus was ineffective. Beyond this interval it evoked a second *NM* spike which was subnormal in size, but full recovery of size had almost occurred at the longest interval in Fig. 3D. At the shortest stimulus intervals there was a lengthened latent period for the *NM* spike, so that the least-response-interval was 1·0 msec. The least-stimulus-intervals and response-intervals have been about 0·8–1·0 msec and 0·9–1·2 msec respectively in those experiments where the second stimulus has been sufficiently strong to excite immediately at the end of the absolutely refractory period.

With a few motoneurones the *NM* spike itself recovered in two stages, being reduced to less than half at very short stimulus intervals and then with slight lengthening of the interval showing a sharp transition almost to full size. Probably motoneurones giving such fractional *NM* spikes have some geometrical feature in the expansion from the constricted segment to the axon hillock which gives a zone of low safety factor for antidromic transmission.

(*b*) *After an NM plus an SD spike*

Fig. 5A shows a typical series of action potentials generated by two antidromic impulses at progressively increasing intervals. With stimulus intervals of 1·25 and 1·35 msec (records 1 and 2) the second volley set up a very small spike response immediately after the end of the first *SD* spike. With lengthening of the stimulus interval to 1·5 msec (record 3) a typical *NM* spike appeared, and finally a stimulus interval of 3·8–4·3 msec (records 8 and 9) was just critical for the generation of an *SD* spike by the second antidromic volley. For example, comparison of record 7 with record 8 indicates that in the latter a small abortive *SD* spike was superimposed upon the *NM* spike, while in record 9 the *SD* spike was developed after a very long axon–soma delay (about 0·4 msec). A full explanation of experimental series such as those of Fig. 5A and B can be attempted only after the systematic investigations described below.

(1) *Stimulus intervals too brief for NM spikes.* As the stimulus interval was shortened, there was always a very sharp transition at a critical interval (about 1·45 msec in this experiment) from the *NM* spike to a very small spike that was often barely detectable (cf. Fig. 5A). A more precise determination of the least-stimulus-interval for evoking an *NM* spike is shown in Fig. 6A, where the second stimulus was at least ten times threshold so that it would excite the motor axon at the very beginning of its relatively refractory period. *NM* spikes were set up with stimulus intervals of 1·10 and 1·13 msec, but not

at 1·07 msec. However, the latent period of the *NM* spike was lengthened with such short stimulus intervals, so that the least-response-interval (measured between the onsets of the first and second *NM* spikes) was 1·25 msec in Fig. 6 A. Accurate measurements of the least *NM* response intervals in three other experiments gave values of 1·23, 1·37 and 1·45 msec.

The shortest stimulus interval at which a second *NM* spike was set up, 1·10 msec, is much longer than the absolutely refractory period of mammalian

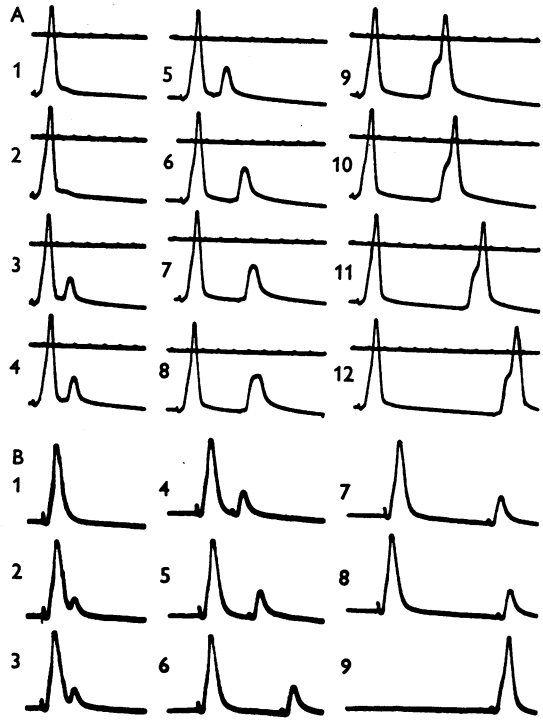

Fig. 5. A: action potentials recorded as in Fig. 2, but set up by double stimulation of the ventral root (two antidromic stimuli) at various time intervals. Time in milliseconds on the reference potential line for zero membrane potential. Resting potential, 72 mV. B: as in A, but in another experiment, the last record showing the control response to the second impulse alone.

A axons, which is usually as brief as 0·5 msec when assessed by the least-stimulus-interval (Gasser & Grundfest, 1936). This discrepancy is not attributable to an inadequate strength of the testing stimulus, or to subnormal temperature of the stimulated ventral roots (cf. Method, Brock *et al.* 1952*a*). Thus it would seem probable that, at intervals shorter than 1·10 msec, the second stimulus had set up a second impulse in the motor axon in the ventral root, but that propagation into the non-medullated segment had been blocked. The very small spikes at the shortest stimulus intervals in Fig. 5 A might be

attributable to such blocked impulses in the medullated segment of the axon. This suggestion has been tested in three experiments by application of a third stimulus to the ventral root. The theoretical basis of this test is that, if the second stimulus had set up an impulse in the medullated axon, then that axon would be made refractory to a third testing stimulus applied shortly thereafter.

In Fig. 7A the stimulus intervals were A_1—1·15 msec—A_2—0·6 msec—A_3 for the three antidromic stimuli. At the A_1–A_3 interval of 1·75 msec, A_3 always set up an *NM* spike when no A_2 stimulus was interpolated (records 3 and 4). When A_2 was interpolated, it always prevented this response (records 1 and 2). Thus it can be concluded that, at an A_1–A_2 interval of 1·15 msec, A_2 had

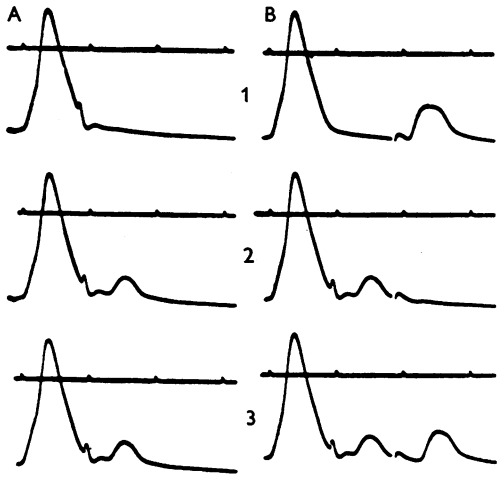

Fig. 6. A: action potentials set up by two antidromic stimuli and recorded as in Fig. 5A, but in another experiment. Time in milliseconds on the reference potential line for zero membrane potential. Resting potential, 66 mV. B: As in A, but for three antidromic stimuli in records 2 and 3, record 1 being for the first and third stimuli only.

set up an impulse in the motor axon and so had made it unresponsive to the A_3 stimulus. The least interval at which the A_2 stimulus set up an *NM* spike was considerably longer in this experiment, 1·25 msec. Similarly it was shown in this experiment that the A_2 stimulus set up an impulse in the motor axon at intervals as short as 1·0 msec.

Still shorter A_1–A_2 intervals were tested in two other experiments. For example, in the two upper records of Fig. 7B, the A_2 stimulus prevented the response to A_3, which was regularly observed for A_1–A_3 alone at that stimulus interval (1·17 msec, cf. record 4). However, the A_2 stimulus no longer prevented the response to A_3 when the A_1–A_2 interval was shortened from 0·62 msec (record 2) to 0·55 msec (record 3). The A_1–A_2 interval of 0·62 msec was critical in this respect, for, as shown in record 5, an A_2 stimulus at this interval failed to prevent a response to A_3 a few seconds later. The A_1–A_3 interval had meanwhile been slightly lengthened to 1·24 msec, but this change should be immaterial. It may be concluded that at 0·55 msec after A_1 the motor axon was still absolutely refractory, while at 0·62 msec it had just recovered therefrom, being excited in one of the two tests. In this experiment a second antidromic stimulus failed to set up an *NM* spike until the A_1–A_2 stimulus interval was lengthened to 1·10 msec (Fig. 6A).

A further control is shown in Fig. 7C where, with an A_1A_2 interval of 0·34 msec, there was no change in the least interval at which the *NM* spike was evoked by a later testing (A_3) stimulus, A_3 being effective at A_1—1·13 msec—A_3 (record 2) and longer intervals and ineffective at A_1—1·09 msec—A_3 (record 1), which agrees closely for the A_1A_2 series of Fig. 6A for this same

motoneurone. Moreover, the least-response intervals are identical, 1·25 msec. Thus when the interpolated antidromic stimulus occurs before the end of the absolutely refractory period, it has no influence on the least interval at which an *NM* response is evoked by a later testing volley, i.e. a brief stimulus applied during the absolutely refractory period does not delay the recovery time as tested by a stimulus applied through these same electrodes.

It may be concluded that in Fig. 7 B for intervals from 0·62–1·10 msec, the second stimulus had set up an impulse in the motor axon, which, however, had failed to invade the non-medullated axon. Presumably blockage had

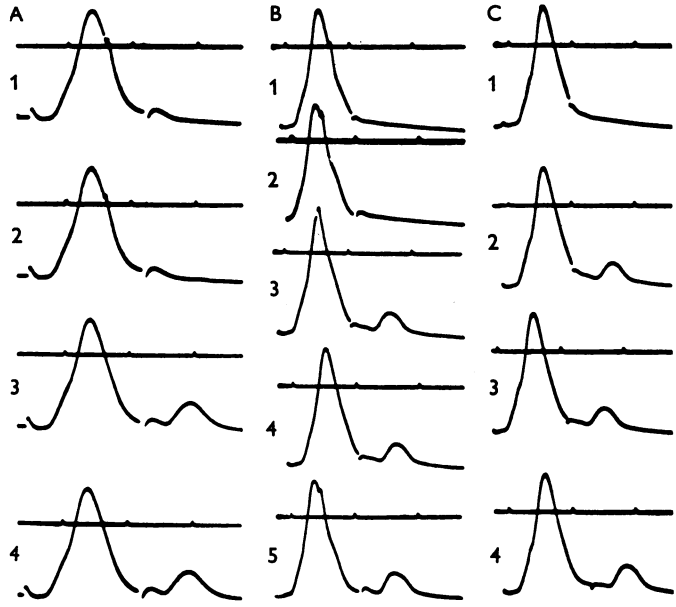

Fig. 7. Action potentials recorded as in Fig. 6 and evoked by two or three antidromic stimuli as described in text. A: in a different experiment from Fig. 6, resting potential, 60 mV. B and C: same motoneurone as Fig. 6, resting potential, 66 mV. B: further description in text. C resembles Fig. 6A except that in all records an antidromic stimulus is interposed at 0·34 msec after the first antidromic stimulus (see text).

occurred at the transition from the medullated to the non-medullated axon. The small spikes set up by the A_2 stimulus in the first two records of Fig. 5A would therefore be attributable to impulses in the medullated axon, which would be expected to give just such small spike-like potentials by electrotonic spread to the soma. Such spikes produced by the medullated segment of the axon will be called '*M*' spikes. They will be further discussed when interpreting the potentials generated by an antidromic tetanus (cf. Figs. 13–15).

Thus after an *SD* spike the propagation from medullated to non-medullated axon breaks down for stimulus-intervals shorter than approximately twice the duration of the absolutely refractory period of the medullated axon. Even after an initial *NM* spike the least-stimulus-interval (0·8–1·0 msec.) was still

surprisingly long. Possibly the non-medullated axon has a longer absolutely refractory period, a suggestion which is supported by the relatively long duration of the *NM* spike (about 0·6–1·0 msec). In general the absolutely refractory period of nerve has usually terminated at the end of the spike (cf. Gasser & Grundfest, 1936; Grundfest, 1940); hence it would seem that an impulse in the medullated axon cannot propagate into the non-medullated axon even when this is in an early stage of its relatively refractory period. It would appear that propagation from the medullated to the non-medullated segment is associated with a low factor of safety, an effect which has been predicted above on theoretical grounds. Thus it would be expected that the critical depolarization of the first part of the non-medullated segment would take some time to be achieved, i.e. that there would normally be a brief delay in conduction. Furthermore, conduction would actually fail to occur when the relative refractoriness of the non-medullated and medullated segments, respectively, had not only raised the critical level of depolarization for transmission from the medullated to the non-medullated fibre, but also had diminished the inward current at the active nodes of the medullated segment (cf. Hodgkin & Huxley, 1952*c*, *d*). Evidence for an increased latent period of any early second *NM* spike has already been presented (cf. Figs. 3D and 6A), an effect which presumably is largely attributable to an increased delay at the transitional region, though of course additional factors would be increased latency at the site of stimulation and slowed conduction velocity.

(2) *Stimulus intervals giving NM spikes.* The critical interval at which the second antidromic impulse set up an *SD* spike has varied widely in the ten motoneurones in which it was determined. In the motoneurones of Fig. 5A it was 3·8–4·55 msec (cf. Fig. 9A). Critical intervals have been observed as brief as 2·5 msec and as long as 50 msec (cf. Fig. 9B). The critical interval has been longer the longer the axon–soma delay for a single volley (cf. Fig. 2). However, in one experiment (Fig. 8) there was a range from 6·1 to 9·0 msec at which antidromic invasion of the soma failed and yet it occurred with intervals from 3·2 to 5·7 msec and also for intervals beyond 9 msec. Other experiments, too, have indicated by the length of the axon–soma delay that there was but little change in the factor of safety for axon–soma transmission with a range of stimulus intervals from 4 to 9 msec (cf. Fig. 5A). It will be shown later that this effect is satisfactorily explained by two overlapping processes which each cause depression of axon–soma transmission.

When the size of the *NM* spike was plotted against the stimulus interval, it showed a very considerable increase, even more than double in some experiments, over the range of very short stimulus intervals, e.g. 1·5–2·6 msec and 1·45–3·6 msec in Fig. 9A and B respectively. There was also a small increase at stimulus intervals just short of the critical interval for soma invasion, which was presumably attributable to the superposition of a small

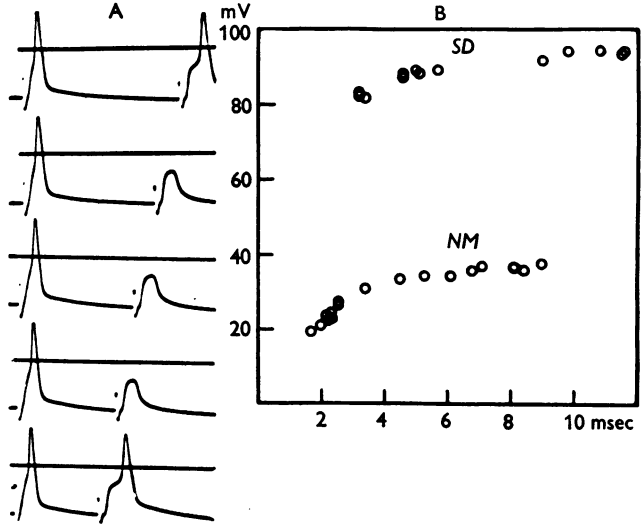

Fig. 8. A: action potentials evoked by two antidromic stimuli as in Fig. 5A, but in another experiment. Spike potential, 94 mV; resting potential probably shown too low on account of drift relative to zero reference potential. Longest interval 9·8 msec. B: plotting of spike potentials of series partly shown in A, the abscissae being stimulus intervals. Note that over range from 3·2 to 5·7 msec there is usually the large *SD* spike, while from then until 9 msec, there is always the small *NM* spike.

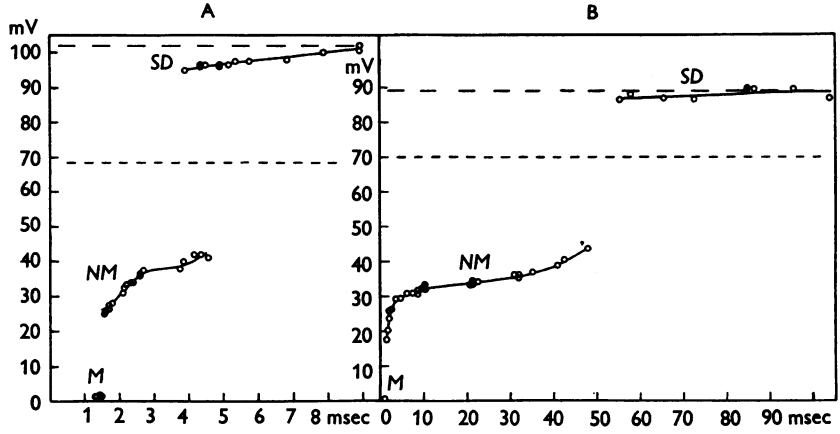

Fig. 9A and B: plotting of antidromic spike potentials against stimulus intervals as in Fig. 8B, but for the two experiments partly illustrated in Fig. 5A and B respectively. Note the different time scales. The responses fall into three distinct groups corresponding to *M*, *NM* and *SD* spikes as indicated.

abortive *SD* spike—the equivalent of a local response (cf. record 8, Fig. 5A). Possibly under such conditions there is a considerable increase in sodium-carrier activity which may later be suppressed by the reversed current flow as suggested above. The additional response so produced is more noticeable as a delayed decline of the *NM* spike than as an increase in its amplitude.

Since, with the usual distortion of the recording, the *NM* spike gradually merged into an after-negativity, it is not possible to give a precise estimate of its duration, but it was always briefer than 1 msec when occurring at intervals

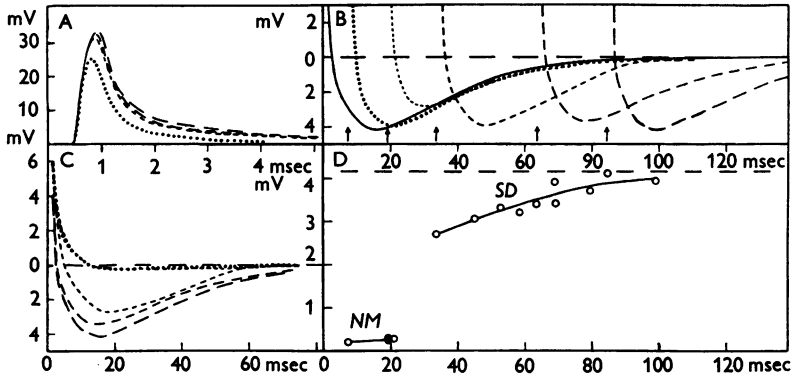

Fig. 10. A: *NM* spikes and after-potentials evoked by a second antidromic impulse at intervals of 2·05 (....), 3·6 (- - - -), 6·15 (– – –) and 8·7 (— — —) msec after a conditioning antidromic response in experiment illustrated by Fig. 5B determined by subtracting response to first volley from the combined response. B: Superimposed tracings of after-potentials evoked by two antidromic impulses in same experiment but with much slower time base and higher amplification. Continuous line gives response to first volley alone (mean of several similar records). Arrows indicate time of second stimulus and the corresponding record is shown about 1 msec thereafter declining from the *NM* (at two shortest intervals) or *SD* spike potentials. C: responses to second antidromic impulse in the records of B as determined by subtraction of the control response from the combined response. Same line convention for B and C. D: Size of positive after-potential evoked by second antidromic impulse is plotted against the stimulus interval for series partly illustrated in B and C. Note discontinuity between *NM* and *SD* responses.

at which there appeared to be little or no addition of an abortive *SD* spike (Fig. 5A, B). In one experiment it was little more than 0·5 msec in duration (Fig. 6, 7B, C).

The time course of the after-negativity is best illustrated by plotting the time course of the potential that the second antidromic response added to the first. As shown in Fig. 10A and C, it closely resembled the after-negativity observed for the *NM* spike set up by a single antidromic volley (Fig. 3A, B, particularly the record at high amplification). Initially the decline was rapid, decay to one-half occurring for example, in 1·3 msec in Fig. 10A, but later there was a considerable lengthening of the half-time to as much as 2·3 msec.

The subtracted curves of Fig. 10C give confirmation of the small size of the positive after-potential for *NM* spikes relative to that for *SD* spikes, an effect already described for the *NM* spike set up by a single antidromic impulse (Fig. 3B, C). For example, after an *NM* spike the positive after-potential was always less than 1% of the spike potential, whereas after an *SD* spike it was about 5% of the spike potential (cf. Brock *et al.* 1952*a*).

The refractory period following an *NM* spike was determined in three experiments by setting up a third antidromic impulse at varying intervals. The least interval between the second and third *NM* spikes (0·97 msec in Fig. 6B) was much less than the least interval between the first and second (1·25 msec in Fig. 6A) obtained for this same motoneurone a few seconds previously. In the other two experiments the respective least intervals between the first and second and the second and third *NM* spikes were respectively 1·23 and 0·98 msec in one and 1·37 and 0·98 msec in the other. These observations are the reverse of those occurring with nerve stimulation, where there is a progressive lengthening of refractoriness and least interval with successive stimulations (Brücke, Early & Forbes, 1941). Presumably this anomaly is attributable to the large *SD* spike associated with the first *NM* response. This suggestion is supported by the relatively brief least-response-intervals (0·9–1·2 msec) also observed after an initial conditioning *NM* spike (cf. Fig. 3D). During and after the first *SD* spike response the non-medullated axon is recovering from refractoriness while being subjected to the powerful catelectrotonic influence of the current flow generated by the *SD* spike. Its refractoriness would thereby be expected to be prolonged in accordance with Blair & Erlanger's (1933) observations on catelectrotonically polarized nerves. Similarly, the refractory period of frog muscle was found to be lengthened by a concurrent end-plate potential (Eccles & Kuffler, 1941).

(3) *Stimulus intervals giving SD spikes.* In the experiments illustrated in Figs. 5A and 8A the *SD* response to the second antidromic volley occurred after an axon–soma delay that was greatly prolonged beyond the control value. No recovery towards normal occurred at such relatively short stimulus intervals. A more complete series is plotted in Fig. 11, where the stimulus interval has been lengthened until the axon–soma delay had virtually been restored to its normal duration. The time course of recovery of axon–soma transmission corresponded approximately to the positive after-potential. A similar correspondence was observed in the two other experiments of this type.

It is relevant that preliminary experiments have indicated that another type of hyperpolarization—that due to inhibition (Brock *et al.* 1952*a*, *b*)—also causes blockage of antidromic invasion of the soma–dendritic membrane and so explains the observations of Renshaw (1946) and Brooks & Eccles (1948).

Figs. 5A and 8A typically show that the *SD* spike set up by the second

volley did not cause as large a reversal of potential as the control *SD* spike. This depression of the spike is not simply attributable to its origin from the trough of the positive after-potential because it was most effective for the *SD* spike that was set up before the positive after-potential developed. Another tentative explanation is that the depression is attributable to the increased axon–soma delay, which would cause the *SD* spike to be less well superimposed on the *NM* spike. However, as soon as the spike and dendrites are invaded by the impulse and have as a consequence approximately the same membrane potential as the active non-medullated axon, the spike in the *NM* segment would cease to contribute appreciably to the spike potential recorded with an intracellular electrode; hence this explanation may be rejected. It is suggested that the most probable explanation would attribute the diminished spike to

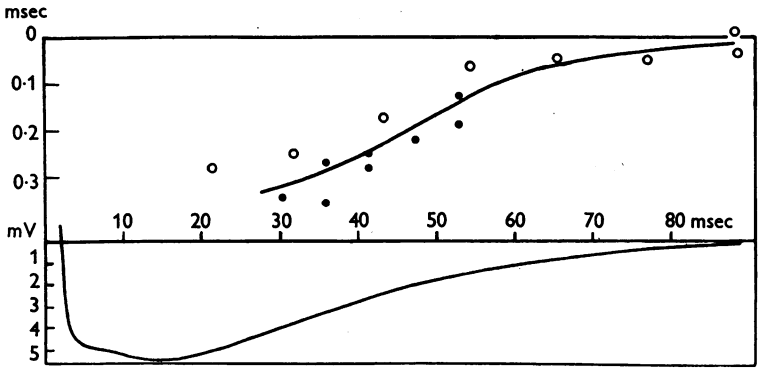

Fig. 11. Points plot variation of axon–soma delay (measured as delay of summit of *SD* spike) for second antidromic impulse at the stimulus intervals given by abscissae. ○ and ●: two experimental series on the same motoneurone. Lower curve is plotted on same time scale and shows time course of positive after-potential following the conditioning antidromic impulse.

the slow recovery of the sodium-carrier mechanism that follows its inactivation subsequent to a brief conditioning depolarization (in this case the conditioning *SD* spike), an effect which was established by Hodgkin & Huxley (1952*c*) for the squid giant axon. A supplementary explanation would be that the *SD* spike potential was depressed because the impulse would spread more slowly and perhaps less extensively over the dendrites. However, Figs. 5A and 8A show typically that, even after the longest axon–soma delays, the *SD* spike potential suffered no lengthening of its time course.

If it is permissible to calculate the after-potential of the second *SD* spike as the potential added to the first *SD* after-potential, Fig. 5A shows that there was a large increase in the size and duration of its negative after-potential. On the same basis the positive after-potential was diminished as shown in the slower recordings at high amplification in Fig. 10B. However, there is a sharp distinction between the diminished, but still considerable, positive after-

potential so determined after an *SD* spike and its virtual absence after an *NM* spike (Fig. 10C). As shown in Fig. 10D the positive after-potential of the second *SD* spike recovered to normal as the stimulus interval was lengthened beyond the duration of the conditioning positive after-potential (cf. Fig. 10B). Observations similar to those following the *SD* spike have been reported with the after-potentials of sympathetic ganglion cells (Eccles, 1935, 1936; Lloyd, 1939), and also of nerve fibres (Gasser, 1937).

III. *Action-potentials generated by repetitive antidromic potentials*

(*a*) *Spike potentials*

As shown in Fig. 12A, when a single antidromic impulse sets up merely an *NM* spike, repetitive stimulation evoked a succession of such spikes, which fell off somewhat in size at the high frequency of 630 per sec. In later stages of such high frequency tetani there may be intermissions in the *NM* spikes, much

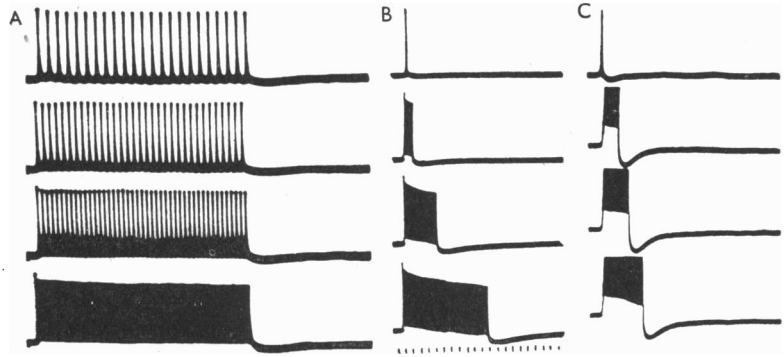

Fig. 12. Intracellular potentials evoked by repetitive antidromic impulses in a motoneurone that gave *NM* spikes only to single impulses. A: brief tetani (140, 205, 280 and 630 per sec) at faster speed to show discrete *NM* spikes, and the early part of the positive after-potential. B: first record is for single impulse, there being progressively longer tetani at 630 per sec with subsequent records. C: as in B at higher amplification with spike summits truncated, but the first record is evoked by three antidromic impulses. Time scale gives 10 msec intervals for B and C.

as illustrated in Figs. 13 and 14. An additional feature with some motoneurones has been intermissions comprising one or more of the fractional *NM* spikes that occasionally have been observed for a second antidromic response at very short stimulus intervals (§ II*a*). The after-potentials will be described in the next section.

Fig. 13 illustrates the repetitive antidromic responses of those motoneurones in which a single antidromic impulse set up an *SD* spike, but a second failed to do so until the stimulus interval was relatively long (cf. Fig. 9B). Each antidromic impulse set up *SD* spikes at the lowest frequencies (13, 20 and 28 per

sec), but after the first few responses this occurred only for every second stimulus at 42 and for every third at 61 per sec. At higher frequencies invasion of the soma occurred still more rarely, and at 280 per sec there were intermissions in the *NM* spikes, an effect which was very evident at the highest frequency (630 per sec). In Fig. 13 the positive after-potential after each *SD* spike is clearly seen, and at the higher frequencies the *NM* spikes were superimposed on the base-line formed by the successive positive after-

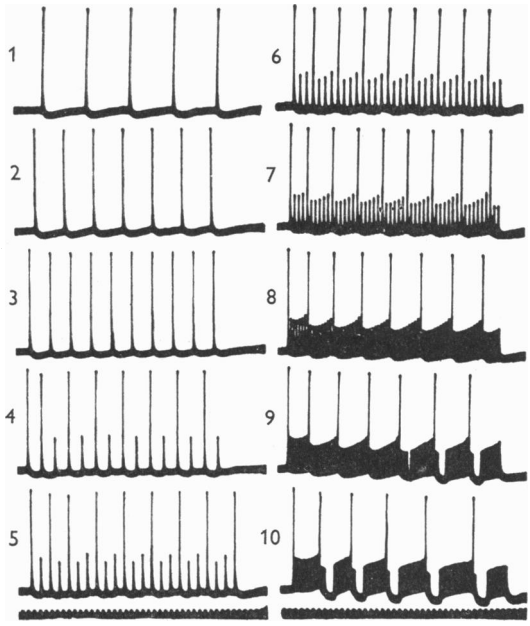

Fig. 13. Intracellular potentials evoked by repetitive antidromic impulses in a motoneurone that gave an *SD* spike to a single antidromic impulse. Approximate stimulus frequencies for traces 1–10 are 13, 20, 28, 42, 61, 91, 140, 205, 280 and 630 per sec respectively. Time scale 10 msec.

potentials. At frequencies above 60 per sec the *NM* spikes were depressed after each *SD* spike, then recovered progressively until eventually they were large enough and the soma sufficiently excitable to allow another *SD* spike to be generated, when the cycle was repeated. At the highest frequencies this sequence was interrupted by the intermissions in the *NM* spikes. As a consequence of the periodic failure of axon–soma transmission, the frequency of the *SD* spikes is maintained at about 20 per sec despite a wide variation in the stimulus frequency.

Fig. 14 illustrates the repetitive responses that have been observed in those preparations where a second antidromic impulse set up an *SD* spike at a relatively short interval. In Fig. 14 the critical interval for *SD* invasion by

a second antidromic impulse was about 4 msec (cf. Figs. 5A and 9A), in contrast to a critical interval of about 20 msec for the motoneurone of Fig. 13. Subsequently, successive stimuli set up *NM* spikes, but the last stimulus failed even to do that at frequencies of 300 and 460 per sec. Longer tetanization of this motoneurone is shown by the records at slower sweep speed (records 5–10). At 150 and 220 per sec an *SD* spike was set up later in the tetanus and possibly it would have been repeated had the tetanus continued longer. At such frequencies the motoneurone of Fig. 14 gave, after the first two *SD* spikes,

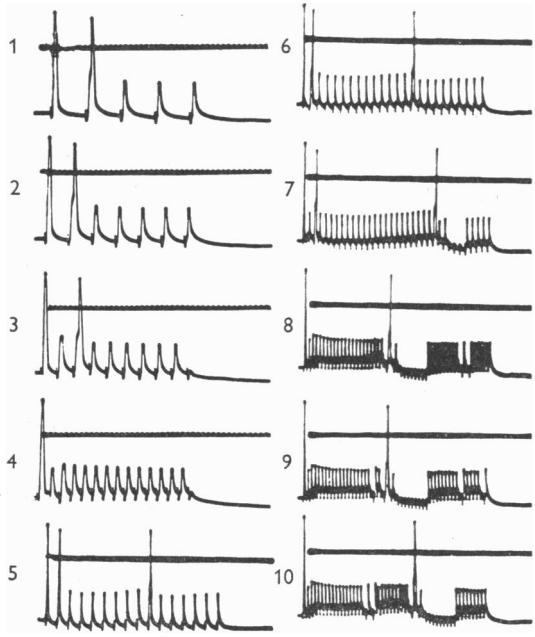

Fig. 14. As in Fig. 13, but for a motoneurone that had a much shorter least-interval for the *SD* response. Records 1–4 are at a faster sweep speed with frequencies of 150, 210, 300 and 460 per sec (fast sweep speed). Records 5–7 at 150, 220 and 300 per sec and 8–10 all at 460 per sec (slow sweep speed). Resting potential as measured from reference potential 65 mV.

responses resembling those of Fig. 13. At 300 per sec also, an *SD* spike was set up later in the series and it was followed by two *NM* spikes and then by an intermission in the *NM* series. At 460 per sec the still more complicated response is illustrated by three records. These are typical of the responses given by most of the neurones that we have investigated and are best described by the following statements.

(*a*) After the onset of a high-frequency antidromic tetanus (frequencies over 300 per sec in our experiments) an *SD* spike is not generated unless there has been an intermission of one or more in the *NM* spike series. However, many intermissions are not thus effective.

(*b*) When an *SD* spike has been set up, the next one or two antidromic stimuli evoke *NM* spikes, but a long intermission then ensues during the positive after-potential that follows the *SD* spike (cf. § III *b*), as may also be observed for the two highest frequencies of Fig. 13.

(*c*) Intermissions thus attributable to the positive after-potential of an *SD* spike are not followed immediately by an *SD* spike as in statement (*a*).

Careful inspection of Fig. 14 reveals that small spikes have still been set up when there has been a failure of the *NM* spikes. These are best seen with the last stimuli in records 3 and 4. Such small spikes would appear to be similar to those which have been set up by the second antidromic impulses at the two shortest stimulus intervals in Fig. 5A, and which have been provisionally identified as *M* spikes generated by impulses in the medullated axon, there being blockage at the medullated–non-medullated junction. This identification is confirmed by observing periods of *NM* intermission at a fast sweep speed

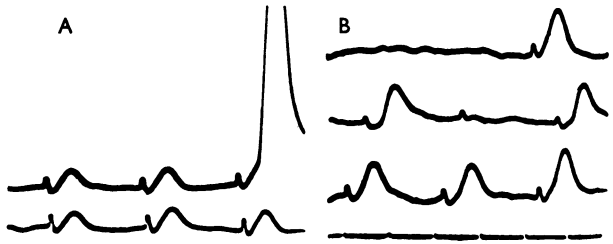

Fig. 15. A: portions of the intracellularly recorded *M* spike potentials evoked by an antidromic tetanus at 470 per sec. The upper record shows an *NM* spike arising from the last *M* spike. B: as in A, but at higher amplification and with weaker stimuli. Upper record shows a single *M* spike and with weak stimulation in second record the second stimulus fails to evoke an *M* spike. Note all-or-nothing character of the *M* spike.

and a higher amplification. As shown in Fig. 15B the *M* spikes were, as expected, about 0·5 msec in duration and showed an all-or-nothing relationship when the strength of the tetanic stimulation was varied. This all-or-nothing character shows that they are not caused by volleys in adjacent motor axons, which often generated a potential of much the same polarity and time course. Thus the intermissions in the repetitive *NM* spike series are attributable to blockage at the junction of the medullated with the non-medullated axon, an effect which has already been observed with a very early second antidromic stimulus (§ II *b* (2)). A partial blockage is indicated in the first record of Fig. 15A by the relatively long interval between the *M* spike and the *NM* spike which it evoked.

(*b*) *Slow potentials*

A repetitive series of *NM* spikes has regularly been followed by a positive after-potential, which, as shown in Fig. 12, builds up to a considerable potential with a high-frequency tetanus. In this respect the *NM* spikes

resemble axonal spikes (Gasser & Grundfest, 1936), and likewise there is evidence that the positive after-potential has an initial phase of about 70 msec (P_1) and a much more prolonged remainder (P_2) (cf. Gasser, 1939).

Each *SD* spike that is set up during the repetitive stimulation is followed by a large positive after-potential (Figs. 13, 14), which is virtually identical with that produced by a single *SD* spike (Brock *et al.* 1952*a*, fig. 5). The full development of the positive after-potential, however, is observed only when there has been an intermission in the *NM* spike series as in Fig. 13, records 9 and 10, and Fig. 14, records 7–10. As soon as the repetitive *NM* spikes returned, there was immediately a diminution of this positive after-potential as revealed by the level of the background potential from which these spikes arose. Presumably this effect is attributable to the after-negativity that followed the *NM* spikes (cf. Figs. 3A, B; 10A, C). This after-negativity can be observed to build up during repetitive series of *NM* spikes in Figs. 13 and 14, though in Fig. 12 there appeared to be a progressive dominance of the positive after-potential. The positive after-potential that ensued on cessation of stimulation at high frequency in Figs. 13 and 14 indicates that the background potential during a repetitive *NM* series was determined by the net effect of the summed after-negativities and positive after-potentials of the *NM* responses.

IV. *Interaction between NM spikes and post-synaptic potentials*

Renshaw (1942) first observed that the negative or 'soma' spike set up by an antidromic volley and recorded by an extracellular micro-electrode is greatly increased by an orthodromic volley. It has been shown (Brooks & Eccles, 1947) that, as the testing interval is lengthened, the facilitation of this soma spike decreases with a time constant of decay that is much the same as with the synaptic facilitation curve (Lloyd, 1946). There is now very convincing evidence that both facilitations are attributable to the partial depolarization (post-synaptic potential) that the orthodromic volley induces in the motoneurones (Brock *et al.* 1952*a*, *b*; Eccles, 1953). According to the hypothesis developed here and elsewhere, this partial depolarization of the soma and dendrites would relieve the axon–soma blockage normally existing in many motoneurones, and hence cause the increased soma spike with extracellular recording.

No opportunity has yet occurred for systematically testing this effect with intracellular recording, but it is easy to arrange for a very similar experiment in which conditioning by an antidromic volley causes a later testing antidromic volley to generate only an *NM* spike (cf. Fig. 5), a post-synaptic potential (p.s.p.) being superimposed in various temporal relationships thereto as illustrated in Fig. 16. Close inspection of Fig. 16 reveals that there is approximate summation of the *NM* spikes and the p.s.p.'s at all phases of interaction. A more accurate study has been made by sweeping the relevant

part of the record faster and at each interval determining, by means of subtraction of the projected records, the potential which the orthodromic volley adds to the A_1A_2 potential (Fig. 17). There is a spike-like addition to the p.s.p. when it is large at the time of the *NM* spike, and a small depression of a p.s.p. set up during the falling phase of an *NM* spike, but this depression has already become virtually ineffective for a p.s.p. generated only 2 msec after the onset of the *NM* spike. At the optimal interval in Fig. 17 the spike-like addition is a full *SD* spike, which is an example of the postulated relief of axon–soma blockage by a p.s.p. This was repeatedly observed when the onsets

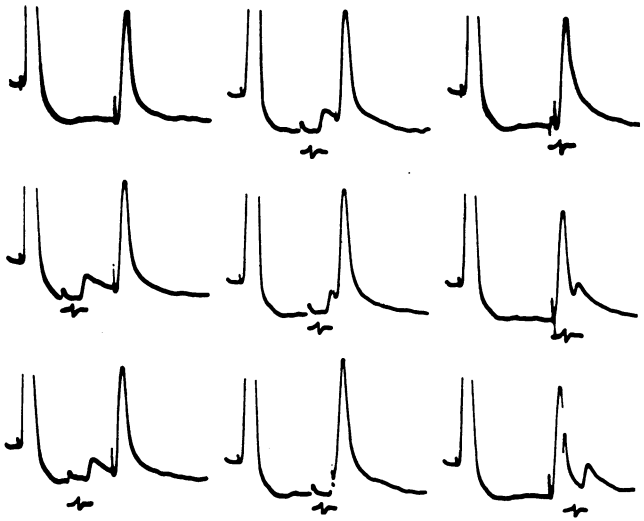

Fig. 16. Intracellular potentials produced in a biceps-semitendinosus motoneurone by two antidromic impulses at 7·2 msec interval and by an orthodromic volley from biceps-semitendinosus nerve which sets up a monosynaptic p.s.p. at various time relationships to the *NM* spike generated by the second antidromic impulse. Immediately below each intracellular record is the action potential of the orthodromic volley as recorded by an electrode on the first sacral dorsal root. The first record is the control response to the two antidromic impulses alone.

of the p.s.p. and the *NM* spike were within 0·1 msec of each other. At other intervals it is suggested that the spike-like addition would be an example of an abortive *SD* spike suppressed by the quenching current from the axon and axon hillock (cf. Fig. 4B). It should be pointed out that the generation of an *SD* spike is due to the superimposed depolarizations of the soma occurring during the *NM* spike and the p.s.p. and one should not be misled by the method of plotting adopted in Fig. 17 to assume that the p.s.p. is more effectively related to the generation of the spike.

The interaction between the p.s.p. and an *NM* spike contrasts strikingly with the effect of an *SD* spike on the p.s.p. as already reported (Brock *et al.*

1952*b*; Eccles, 1953). An *SD* spike virtually destroyed all existing p.s.p., and no appreciable p.s.p. could be built up until late on the decline of the *SD* spike. Furthermore, there is a much deeper and more prolonged (at least for 10 msec) depression of the p.s.p. after an *SD* spike than after an *NM* spike, and the time constant of decay of the p.s.p. is also much briefer after an *SD* spike. All

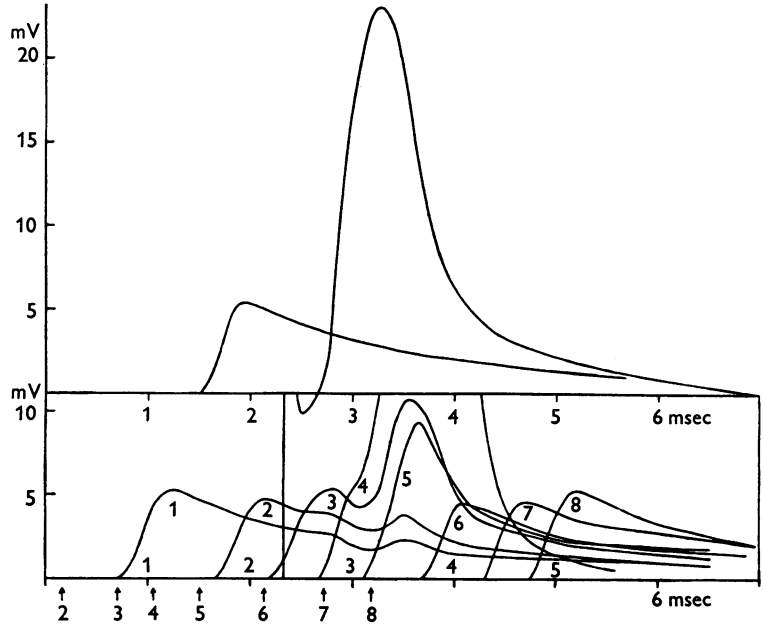

Fig. 17. Tracings of action potentials from same experimental series as Fig. 16, but with faster time base. In the upper section are the control records of the *NM* spike and the p.s.p. which the orthodromic volley produces after conditioning by the first antidromic volley alone, the orthodromic stimulus being applied at zero on the time scale. In the lower section are plotted the potentials added by the orthodromic volley when it occurs at eight different times relative to the *NM* spike of the second antidromic volley which is fixed at the same time as the control above. The arrows 2–8 mark the times of the orthodromic stimuli that evoke the potentials labelled 2–8 respectively. Stimulus 1 is beyond the left of the figure. The perpendicular line gives the fixed time of the second antidromic stimulus. Note that coincidental with the *NM* spike there is a spike-like addition to the p.s.p., which increases from records 1 to 3 to give a full *SD* spike at 4 and then declines to a small spike at 5. Further description in text.

these differences are to be expected if the membrane activated during the *NM* spike is virtually restricted to a part of the motoneurone that is not actively contributing to the p.s.p., i.e. on which there are very few if any excitatory synapses. On the other hand, the *NM* spike must arise in a part of the motoneurone that is very close to the synaptically activated surface of the soma and dendrites, for it can effectively sum with the p.s.p. to give a spike

and it exerts a slight depressant effect on a p.s.p. generated on its falling phase (Fig. 17B, 6 and 7). It has already been suggested that during the decline of the *NM* spike the large outward potassium current of the membrane that had been activated by the *NM* spike was very effectively aiding, by means of local current flow, the repolarization of the neuronal membrane, an effect which would account for the observed depressions of the p.s.p. Thus the experimental evidence is fully accounted for by the hypothesis that the *NM* spike is generated by an impulse in the non-medullated axon and the axon hillock, and it effectively excludes any postulate that the *NM* spike is generated further centrally in the motoneurone, e.g. in the soma.

DISCUSSION

Antidromic potentials

With intracellular recording from motoneurones an invariable finding has been that antidromic impulses set up spike-like potentials which fall into three sharply defined classes, the *SD*, *NM* and *M* spikes. Before discussing generally the problem of antidromic transmission into motoneurones, it is important to examine critically all the experimental evidence that bears on the identification of these three types of spikes with the antidromic invasion of specific parts of a motoneurone.

It was convenient to postulate earlier that the *NM* spike is generated when the antidromic invasion spreads over the non-medullated segment of the axon and some distance over the axon hillock, and that the *SD* spike is produced by the extension of this invasion to the soma and dendrites. The evidence supporting these identifications may now be assembled.

In the first place it is certain that the micro-electrode lies within some part of a motoneurone because initially it records a resting potential, which is itself diminished or reversed by the spike potential generated on antidromic activation via the ventral root. Furthermore, it may be assumed that in our experiments the micro-electrode lies in some part of the soma or adjacent large dendritic branches, for the soma offers by far the largest target, and with our imperfect fixation other parts of the motoneurone, e.g. the finer dendritic branches or the axon, would be unlikely to accommodate the micro-electrode for more than a few seconds. Such brief insertions are sometimes encountered. Since the *SD* spike is so large that it produces reversal of the resting membrane potential, it must be caused by an impulse in the membrane immediately adjacent to the micro-electrode, i.e. in the soma membrane. Histologically the dendrites appear merely as large extensions of the soma, and, on the local-circuit theory of impulse propagation, it would be expected that once the antidromic impulse had invaded the soma, it would rapidly spread over the large dendritic branches. This expectation receives convincing experimental

support from the finding that an *SD* spike causes virtually complete destruction of a pre-existent post-synaptic potential (Brock *et al.* 1952*b*; Eccles, 1953). The *SD* spike must therefore invade those parts of the post-synaptic membrane which are depolarized by the excitatory action of presynaptic impulses and which are sufficiently close to the intracellular electrode, i.e. the membrane of the soma and large dendritic branches.

On the other hand, the *NM* spike causes very little destruction of a pre-existent post-synaptic potential (Figs. 16, 17), and quite large post-synaptic potentials can be superimposed upon an *NM* spike. However, summation of these two depolarizations is likely to be complicated by the generation of an *SD* spike (Fig. 17), which in turn destroys the post-synaptic potential. It may be concluded that, in generating the *NM* spike the antidromic impulse must be blocked before it invades an appreciable part of the synaptically innervated zone of the motoneurone, i.e. the soma and dendrites. Yet the relatively large size of the *NM* spike shows that the invaded membrane is closely adjacent to the micro-electrode in the soma (cf. Fig. 4A). It has already been pointed out that, according to the local-circuit theory of impulse propagation, transmission from the constricted non-medullated segment into the conical expansion of the axon hillock to soma would have a low factor of safety, hence all the available evidence indicates that the *NM* spike is produced when the antidromic impulse is blocked somewhere in the axon hillock. The abortive addition to the *NM* spike (Fig. 17) that occurs under conditions just short of its growth to an *SD* spike is then satisfactorily attributed to a local response of the soma–dendritic membrane.

The small size of the *M* spike, its short refractory period, brief duration, all-or-nothing character, ability to follow high frequencies, and its location immediately peripheral to the membrane giving the *NM* spike make its location in the medullated segment very probable.

Additional evidence for the localization of the *NM* and *SD* spikes is provided by the positive after-potentials, which are always relatively much larger after *SD* spikes than after *NM* spikes, being on the one hand never less than about 3% of the *SD* spike height and on the other never more than 1% of the *NM* spike height. This latter value is of the same order as with peripheral mammalian axons (Gasser & Grundfest, 1936; Grundfest, 1940); hence further experimental support is provided for the axonal origin of the *NM* spikes. The large positive after-potential following the *SD* spike undoubtedly causes depression of the invasion by a second antidromic impulse as shown by failure or delay of the *SD* spike (cf. Figs. 9 and 11; Brooks *et al.* 1950; Lloyd, 1951*a*), and presumably it also causes the concurrent depression of the synaptically evoked discharge from the motoneurone (Brooks *et al.* 1950; Lloyd, 1951*a*). Thus the *SD* spike is again identified with the synaptically activated membrane of the motoneurone.

It now remains to consider whether the other experimental investigations on the *NM* spike can be satisfactorily explained. Explanations have already been offered for the large size of the *NM* spike, the relatively long refractory period after a conditioning antidromic impulse, particularly one that evokes an *SD* spike, and the large after-negativity that is often observed (Figs. 2B, 10A, C).

In Fig. 9, after a conditioning antidromic impulse, the *NM* spike set up by a later testing antidromic impulse is small at the shortest intervals and increases to a plateau level with lengthening of the testing interval. Presumably the small size of the *NM* spike is partly attributable to the usual conditions obtaining for a membrane during relative refractoriness (Hodgkin & Huxley, 1952*d*): partial inactivation of the sodium-carrier mechanism; high level of potassium conductance. Both these effects would diminish the inward current during a spike response of the non-medullated membrane (cf. Fig. 4A). But, after an *SD* spike, an additional factor would arise on account of the high potassium conductance of the soma–dendritic membrane, which would effectively diminish the depolarizing effect of the outward currents that flow through this membrane and that give, as a consequence, the *NM* spike as actually recorded (cf. Fig. 4A).

Axon–soma transmission

When there is antidromic invasion of the soma and dendrites, there is wide variation in the delay at the axon–soma junction from about 0·05 to 0·4 msec. Presumably this delay is largely occupied in the depolarization of the soma by extrinsic current flow until a critical level is attained for generating an impulse in the soma. After about 0·3 msec there will be a rapid decline of these extrinsic currents, which soon reverse (Fig. 4B); hence if the critical depolarization is not attained in about 0·4 msec, it never will be attained, i.e. the observed value of 0·4 msec would be expected to be the longest possible axon–soma delay. Local responses of the soma membrane adjacent to the axon hillock would of course tend to prolong the soma–dendritic depolarization despite the decline and reversal of the extrinsic currents (cf. Figs. 3A, 5A). The shortest values of axon–soma delay would be expected to occur when there is the largest safety factor for transmission. As predicted, axon–soma transmission is then restored at very short intervals after a conditioning antidromic volley (cf. Figs. 5A and 9A).

As shown in Fig. 8, as the testing interval is lengthened, the phase of blockage of axon–soma transmission (as shown by the *NM* spikes) may have a brief phase of axon–soma transmission superimposed upon it (at stimulus intervals of 3·2–5·7 msec in Fig. 8B). The final recovery of axon–soma transmission was not observed until 9 msec. This complex behaviour is satisfactorily explained by the combination of two factors depressing axon–soma transmission:

relative refractoriness of the axon and soma at the shortest test intervals; hyperpolarization of the soma membrane due to the positive after-potential at longer intervals. In Fig. 8B there has been adequate recovery from the relative refractoriness by 3·2 msec and the after-negativity did not reverse to the positive after-potential until about 6 msec. Thus over the intermediate range from 3 to 6 msec the restoration of transmission is attributed to the combined effects of partial recovery from relative refractoriness and the relative supernormality associated with the negative after-potential. Beyond 6 msec the subnormality associated with the positive after-potential would cause further blockage of transmission. Presumably it exerts this effect by summation with a residuum of relative refractoriness because the final recovery of transmission at about 9 msec occurs during the maximum of the positive after-potential and must therefore be attributed to recovery from this residual relative refractoriness, though possibly accommodation to the positivity may also be a factor. Axon–soma transmission is still very delayed, and the depressant action of the positive after-potential throughout its whole duration has been well illustrated by the shortening of this transmission time to normal along a recovery curve that parallels the positive after-potential (cf. Fig. 11).

Possibly these observations on single motoneurones provide an explanation of the transient recovery of some motoneurones after antidromic activation as observed experimentally on the whole motoneurone population (cf. § iv of the introduction). With intracellular recording we have never observed the alternative condition there suggested, namely production of an *SD* response when there is facilitation of a second *NM* spike by the residuum of soma depolarization following a conditioning *NM* spike.

Conclusions

It is now possible to give in summary form the conclusions relating to the antidromic responses of motoneurones and the properties of motoneurones derivable therefrom.

(1) Under normal conditions propagation occurs from the medullated to the non-medullated segment, but the low safety factor that would be expected for this transmission causes blockage to occur during rapid repetitive stimulation, especially if the non-medullated segment is subjected to the hyperpolarizing influence of the current flowing during the positive after-potential of the soma–dendritic membrane (cf. Figs. 13 and 14).

(2) As would be expected from the local-circuit theory of propagation, a still lower safety-factor occurs for the propagation from the constricted non-medullated segment outwards over the conical expansion of the axon hillock to soma. Even for motoneurones having the highest safety-factors, there is a phase of slowed propagation which appears as an axon–soma delay of 0·05–0·4 msec, while with other motoneurones there is axon–soma blockage.

(3) Axon–soma blockage occurs in all motoneurones shortly after a conditioning antidromic volley. At brief stimulus intervals this blockage is attributable to relative refractoriness, and at longer intervals to the positive after-potential of the soma–dendritic membrane, which is about 100 msec in duration. These depressant effects overlap over a range that usually extends from about 4 to 10 msec. Axon–soma blockage has also been observed when the soma–dendritic membrane is sufficiently hyperpolarized by synaptic inhibitory action.

(4) Facilitation of axon–soma transmission is produced when the soma–dendritic membrane is depolarized by synaptic excitatory action, i.e. during the post-synaptic potential, blockage being relieved (Fig. 17) and delay being shortened.

(5) Invasion of the soma–dendritic membrane is normally all-or-nothing, the spike potential so generated being about 1 msec in duration and terminating sharply in the after-negativity. However, under conditions just critical for transmission, there may be a small partial invasion of the soma membrane, a type of local response.

(6) During the soma–dendritic spike there is the usual reversal of membrane potential to about 30 mV external negativity, and thereafter a negative and positive after-potential. The latter is larger than in peripheral axons by a factor of five to ten.

(7) When the antidromic impulse is blocked at the axon–soma junction, there is a considerable depolarization (about 30 mV) of the soma–dendritic membrane. This depolarization is much larger than the normal threshold level for generation of a spike (about 10 mV), a discrepancy which has been attributed to the strong extrinsic repolarizing current that rapidly follows the initial depolarizing current.

(8) In general the responses produced during antidromic invasion of a motoneurone are largely explicable by the anatomical features of the pathway, in particular by the geometry of the conical expansion at the axon–soma transition. But some degree of physiological specialization must be postulated for the soma–dendritic membrane, which has a spike duration considerably longer than the axon and a much larger positive after-potential.

General discussion

By making five assumptions, Barakan *et al.* (1949) explained the electrical responses evoked by an antidromic volley under various conditions and recorded throughout the cross-section of the spinal cord by a penetrating micro-electrode. Four of these five assumptions are contained in the above set of conclusions, and there is even very close quantitative agreement in the respective values for axon–soma delay and soma spike duration. The remaining

assumption concerned propagation over the dendritic terminals, which could not at present be tested by intracellular recording. In particular, Barakan *et al.* attributed the lability of the negative spike as recorded in the region of the motor nucleus to a lability of axon–soma transmission exactly as formulated in conclusions (2), (3) and (4) above.

Similarly, the conclusions of Brooks *et al.* (1950) have been substantiated by the intracellular records where these have been applicable (particularly conclusions (3) and (6)).

Recently, Lloyd (1951*a*, *b*) has reached some very different conclusions from an analysis of the potentials which are generated by an antidromic volley and recorded mainly from the surface of the spinal cord. For example, it is concluded that axon–soma delay and blockage is not established as an important factor, that the lability of the main antidromic spike is due to a high degree of 'subtlety' of conduction in dendrites (Lloyd, 1951*a*), and that, during the antidromic after-potentials, current in the external circuit flows from the somata and dendrites to axons for about 45 msec and then reverses to flow from axons to somata and dendrites for a further 75 msec (Lloyd, 1951*a*, *b*). In a brief commentary it is possible to indicate how some of these differences have arisen.

First, Lloyd has invariably employed a maximum antidromic volley in a ventral root, and hence a complex pattern of discrete nuclei of motoneurones will be activated (cf. Marinesco, 1904; Romanes, 1951). Lloyd (1951*a*) interprets this whole pattern as being simply equivalent to a giant motoneurone occupying the whole ventral horn. It should be pointed out that in a previous analysis of the potential fields generated by an antidromic volley, Barakan *et al.* (1949) invariably employed an antidromic volley restricted to the axons of a relatively discrete nucleus of motoneurones. Such conditions offer much more justification for the simplification to a single giant motoneurone.

Secondly, Lloyd (1951*a*) attributes his '*b*' wave to antidromic invasion of the cell body (soma in our terminology), whereas his observations accord with ours if the '*b*' wave is due to the antidromic invasion of the non-medullated segment and the axon hillock, i.e. if his '*b*' wave is equivalent to our *NM* spike. His identification is based on three attributes of the '*b*' wave: its localization in the region of the ventral horn; its relatively long refractory period with a least interval of about 1 msec longer than the medullated axon; its sensitivity to the depolarizing influence of asphyxia. All of these attributes would obtain for the non-medullated axon, for even if it were less rapidly depolarized by asphyxia than the soma and dendrites, it would be very effectively depolarized by the flow of current into such primarily depolarized areas. It should be noted that Lloyd's rejection of the concepts of axon–soma delay and blockage is based almost exclusively on the identification that he has given to his '*b*' wave,

and that consequently he has to attribute the lability of the antidromic responses to dendritic conduction.

If the '*b*' wave is thus attributable to the non-medullated axon, to what is Lloyd's '*i*' wave attributable? Since the least-response-interval corresponds approximately to the medullated axon, and since it is only detectable by a micro-electrode in the ventral horn, it seems likely that it is generated by impulses in medullated axons within the ventral horn, particularly those traversing to the most dorsally placed motoneurones.

Thirdly, from an analysis of the after-potentials that follow an antidromic volley, Lloyd (1951*b*) derives the temporal pattern of after-currents that after 45 msec flow in the external circuit in the opposite direction from the currents that would be generated by the after-potentials recorded in this paper. Intraneuronal recording establishes that the *SD* spike is followed by a large positive after-potential that continues for 100–120 msec, while after the *NM* spike the positive after-potential runs much the same time course, but is at most one-fifth the size (relative to the respective spike potentials). Thus, for the whole duration of the after-potential, after-currents flow in the external circuit from the soma to the axon and there can be no doubt that the positive after-potential of the soma and dendrites is adequate both in intensity and duration to account for the depression of the antidromically activated motoneurone as tested either by a second antidromic volley or by an orthodromic volley. Unfortunately, it has not been possible to offer an alternative explanation for Lloyd's (1951*b*) elegant experiments on the antidromic after-potentials and after-currents. But it must be pointed out that for currents flowing between the soma and the axon the intracellular micro-electrode is a much more sensitive (about 100 times) and direct indicator than is the external micro-electrode, particularly when account is taken of the complex pattern of motoneurone distribution in the ventral horn and the external fields of current which will probably flow to dendrites as well as to axon.

The analysis of externally recorded antidromic potentials is of importance because it would seem to be the only method of determining the reactions of the finer dendrites and the dendritic terminals. However, this analysis must if possible be done on the responses of single motoneurones from which intracellular potentials have also been recorded. The antidromic responses of the whole assemblages of motoneurones in the ventral horn would appear to give fields of current which are topographically so complex that, if external focal recording only is employed, the behaviour of a single motoneurone cannot be derived therefrom by even the most exacting analytical procedures.

SUMMARY

1. Intracellular recording from motoneurones in the lumbar region of the cat's spinal cord has provided evidence on most of the controversial issues concerning antidromic responses of motoneurones.

2. The geometry of the antidromic pathway indicates that low safety-factors for transmission would occur at the medullated–non-medullated junction and at the axon–soma junction, and on this basis detailed explanations are given for most of the experimental observations. With blockage at the latter site there is a simple *NM* (non-medullated) spike of about 30–40 mV, in contrast to the *SD* (soma–dendritic) spike of up to 100 mV on full antidromic invasion. With blockage at the former site there is a very small *M* (medullated) spike of about 1 mV.

3. When axon–soma transmission normally occurs, it is associated with a delay of 0·05–0·4 msec. Depression by the refractory period or the positive after-potential following a previous *SD* spike causes blockage of transmission, or at least lengthening of the delay, 0·4 msec being the upper limiting value. Likewise medullated–non-medullated transmission is blocked by refractoriness or hyperpolarization of the non-medullated segment.

4. In addition to the voltage differences which are explicable by the assumed location of the micro-electrode in the soma, the *SD* spike differs from the *NM* spike in its longer duration (about 1 msec) and in the positive after-potential which is larger, relative to the spike potential, by a factor of five to ten. The currents flowing during and after an *NM* spike are correlated with the electrical events in the soma, in particular with the generation of an *SD* spike.

5. Detailed descriptions are given of the *SD*, *NM* and *M* spikes set up by two antidromic impulses at various intervals and by repetitive trains of antidromic impulses at various frequencies.

6. The interaction of the *NM* spike with the post-synaptic potential is investigated, depolarization produced by the latter aiding, as would be expected, in antidromic transmission.

REFERENCES

BARAKAN, T. H., DOWNMAN, C. B. B. & ECCLES, J. C. (1949). Electric potentials generated by antidromic volleys in quadriceps and hamstring motoneurones. *J. Neurophysiol.* **12**, 393–424.

BLAIR, E. A. & ERLANGER, J. (1933). A comparison of the characteristics of axons through their individual electrical responses. *Amer. J. Physiol.* **106**, 524–564.

BROCK, L. G., COOMBS, J. S. & ECCLES, J. C. (1951). Action potentials of motoneurones with intracellular electrode. *Proc. Univ. Otago med. Sch.* **29**, 14–15.

BROCK, L. G., COOMBS, J. S. & ECCLES, J. C. (1952*a*). The recording of potentials from motoneurones with an intracellular electrode. *J. Physiol.* **117**, 431–460.

BROCK, L. G., COOMBS, J. S. & ECCLES, J. C. (1952*b*). The nature of the monosynaptic excitatory and inhibitory processes in the spinal cord. *Proc. Roy. Soc.* B, **140**, 169–176.

BROCK, L. G., COOMBS, J. S. & ECCLES, J. C. (1953). Antidromic propagation of impulses into motoneurones. *The Spinal Cord*, pp. 120–129. Ciba Foundation Symposium. London: Churchill.

BROOKS, C. McC., DOWNMAN, C. B. B. & ECCLES, J. C. (1950). After-potentials and excitability of spinal motoneurones following antidromic activation. *J. Neurophysiol.* **13**, 9–38.

BROOKS, C. McC. & ECCLES, J. C. (1947). Electrical investigation of the monosynaptic pathway through the spinal cord. *J. Neurophysiol.* **10**, 251–274.

BROOKS, C. McC. & ECCLES, J. C. (1948). Inhibition of antidromic responses of motoneurones. *J. Neurophysiol.* **11**, 431–444.

VON BRÜCKE, E. T., EARLY, M. & FORBES, A. (1941). Recovery of responsiveness in motor and sensory fibres during the relatively refractory period. *J. Neurophysiol.* **4**, 80–91.

CAJAL, S. R. (1909). *Histologie du système nerveux de l'homme et des vertébrés*, Vol. 1. Paris: Maloine.

ECCLES, J. C. (1935). Slow potential waves in the superior cervical ganglion. *J. Physiol.* **85**, 464–501.

ECCLES, J. C. (1936). Synaptic and neuro-muscular transmission. *Ergebn. Physiol.* **38**, 339–444.

ECCLES, J. C. (1950). The responses of motoneurones. *Brit. med. Bull.* **6**, 304–311.

ECCLES, J. C. (1952). The electrophysiological properties of the motoneurone. *Cold Spr. Harb. Symp. quant. Biol.* **17**, 175–183.

ECCLES, J. C. (1953). *The Neurophysiological Basis of Mind.* Oxford: Clarendon Press.

ECCLES, J. C. & KUFFLER, S. W. (1941). The endplate potential during and after the muscle spike potential. *J. Neurophysiol.* **4**, 486–506.

ECCLES, J. C. & PRITCHARD, J. J. (1937). The action potential of motoneurones. *J. Physiol.* **89**, 43–45*P*.

GASSER, H. S. (1937). In ERLANGER J. & GASSER H. S., *Electrical Signs of Nervous Activity.* University of Pennsylvania Press.

GASSER, H. S. (1939). Axons as samples of nervous tissue. *J. Neurophysiol.* **2**, 361–369.

GASSER, H. S. & GRUNDFEST, H. (1936). Action and excitability of mammalian A fibres. *Amer. J. Physiol.* **117**, 113–133.

GRUNDFEST, H. (1940). Bioelectric potentials. *Annu. Rev. Physiol.* **2**, 213–242.

HODGKIN, A. L. & HUXLEY, A. F. (1952*a*). Currents carried by sodium and potassium ions through the membrane of the giant axon of *Loligo*. *J. Physiol.* **116**, 449–472.

HODGKIN, A. L. & HUXLEY, A. F. (1952*b*). The components of membrane conductance in the giant axon of *Loligo*. *J. Physiol.* **116**, 473–496.

HODGKIN, A. L. & HUXLEY, A. F. (1952*c*). The dual effect of membrane potential on sodium conductance in the giant axon of *Loligo*. *J. Physiol.* **116**, 497–506.

HODGKIN, A. L. & HUXLEY, A. F. (1952*d*). A quantitative description of membrane current and its application to conduction and excitation in nerve. *J. Physiol.* **117**, 500–544.

HUXLEY, A. F. & STÄMPFLI, R. (1951). Effect of potassium and sodium on resting and action potentials of single myelinated nerve fibres. *J. Physiol.* **112**, 496–508.

LLOYD, D. P. C. (1939). The origin and nature of ganglion after-potentials. *J. Physiol.* **96**, 118–129.

LLOYD, D. P. C. (1943). The interaction of antidromic and orthodromic volleys in a segmental spinal motor nucleus. *J. Neurophysiol.* **6**, 143–151.

LLOYD, D. P. C. (1946). Facilitation and inhibition of spinal motoneurons. *J. Neurophysiol.* **9**, 421–438.

LLOYD, D. P. C. (1951*a*). Electrical signs of impulse conduction in spinal motoneurons. *J. gen. Physiol.* **35**, 255–288.

LLOYD, D. P. C. (1951*b*). After-currents, after-potentials, excitability, and ventral root electrotonus in spinal motoneurons. *J. gen. Physiol.* **35**, 289–321.

LORENTE DE NÓ, R. (1947). Action potential of the motoneurons of the hypoglossus nucleus. *J. cell. comp. Physiol.* **29**, 207–288.

MARINESCO, G. (1904). Recherches sur les localisations motrices spinales. *Sem. médicale*, **24**, 225–231.

RENSHAW, B. (1942). Effects of presynaptic volleys on spread of impulses over the soma of the motoneuron. *J. Neurophysiol.* **5**, 235–243.

RENSHAW, B. (1946). Observations on interaction of nerve impulses in the grey matter and on the nature of central inhibition. *Amer. J. Physiol.* **146**, 443–448.

ROMANES, G. J. (1951). The motor cell columns of the lumbo-sacral spinal cord of the cat. *J. comp. Neurol.* **94**, 313–363.